Pinning and sliding of tethered monolayers on disordered substrates

Carlo Carraro[1] and David R. Nelson[2]
[1]*Department of Chemistry, University of California, Berkeley, California 94720*
[2]*Department of Physics, Harvard University, Cambridge, Massachusetts 02138*
(Received 24 July 1996; revised manuscript received 7 January 1997)

We study the statistical mechanics and dynamics of crystalline films with a fixed internal connectivity on a random substrate. Defect free triangular lattices exhibit a sharp transition to a low temperature glassy phase with anomalous phonon fluctuations and a nonlinear force-displacement law with a continuously variable exponent, similar to the vortex glass phase of directed lines in 1+1 dimensions. The periodicity of the tethered monolayer acts like a filter which amplifies particular Fourier components of the disorder. However, the absence of annealed topological defects like dislocations is crucial: the transition is destroyed when the constraint of fixed connectivity is relaxed and dislocations are allowed to proliferate.
[S1063-651X(97)10707-3]

PACS number(s): 63.20.Mt, 46.30.Pa, 68.35.Rh

I. INTRODUCTION

The pinning of elastic media subjected to external forces is a subject of considerable interest in connection with a variety of phenomena, ranging from tribology to epitaxial surface growth to transport of flux line arrays in type II superconductors [1]. High temperature superconductors are especially interesting in this respect because of the simultaneous presence of large thermal fluctuations and of quenched disorder. Much effort has been devoted to the study of 1+1-dimensional models, which are models of vortex lines confined to a plane [2,3] [see Fig. 1(a)]. Although some quantitative questions have yet to be answered satisfactorily, a clear qualitative picture of the physics involved has emerged, which can be summarized as follows: the 1+1-dimensional flux array, subjected to external point disorder, displays a transition, at some temperature T_g, between a high temperature regime, dominated by thermal fluctuations, and a low temperature regime, where the behavior of the system is controlled by a line of fixed points. The low temperature phase is a disorder-dominated phase, where the elastic system is pinned. Pinning affects both static correlations and dynamic responses in a nontrivial way, giving rise to nonlinear current-voltage characteristics. Crucial to pinning is the discrete nature of the elastic system, which, roughly speaking, acts as a Fourier filter for components of disorder on length scales corresponding to the lattice spacing (i.e., the distance between flux lines).

The question naturally arises whether coherent amplification of the disorder (assumed to exist at all physically relevant wave lengths) is instrumental to the pinning of a vortex array; that is, it is important to question the role of long range crystalline order of the array in selecting out particular Fourier components of the pinning potential. *This feature is built into the* 1+1*-dimensional vortex line model*, which possesses *algebraic* crystalline order at all nonzero temperatures *and* is also topologically perfect. The topological perfection arises for vortex lines because the average magnetic field is parallel to the plane, and thus the lines cannot terminate in the plane, and their labeling in a perfect crystalline sequence is always unambiguous.

Alternative two-dimensional models of elastic solids can be considered, which allow for topological defects, such as dislocations. These are 2+0-dimensional models [see Fig. 1(b)]. For vortices in superconductors, the average magnetic field must then be perpendicular to the plane of the film, and defects leading to multivalued displacements of the vortices are allowed, as they are in many other experimental situations. Additional experimental realizations include colloidal crystals [4], amphiphillic monolayers or bilayers composed of lipid molecules (possibly polymerized) [5], electrons in semiconductor heterostructures [6], and magnetic bubble arrays [7]. The constraint of fixed nearest neighbor connectivity could be enforced in some cases by polymerization or, more generally, simply by large kinetic barriers to particle

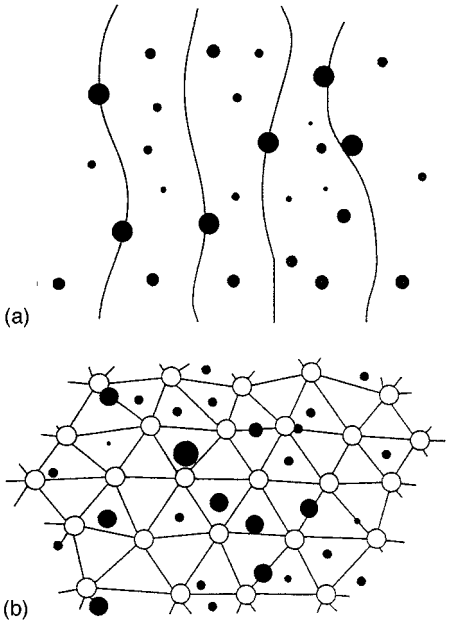

FIG. 1. (a) Directed lines in 1+1 dimensions subjected to random point pinning due to a disordered substrate. (b) Tethered network of particles in 2+0 dimensions subjected to random point pinning due to a disordered substrate.

exchanges at low temperature. These systems can be topologically perfect, or else can be subject to either quenched or annealed internal defects, in addition to the external pinning potential.

The goal of the present work is to develop the theory of pinned two-dimensional crystals within the framework of two-dimensional elasticity theory. For the case of a topologically perfect crystal of identical tethered particles, subjected to thermal fluctuations and quenched pinning, we show here that the behavior is qualitatively similar to the 1+1-dimensional model, displaying, e.g., a sharp phase transition to a low temperature pinned phase. Although the detailed results for the transition temperature and exponents are certainly interesting, we should emphasize that the possibility of topological defects introduces significant modifications.

Annealed dislocations destroy positional quasi-long-range order in two-dimensional crystals above some finite melting temperature T_M, where a liquid crystalline ''hexatic'' phase exists, with algebraic long range order in the bond angle [8]. As will be shown below, the melting temperature is always smaller than T_g, so that a two-dimensional crystal is always melted at the temperature below which pinning disorder would become relevant for a topologically perfect solid (i.e., dislocations are a relevant perturbation at T_g). Thus the transition of a topologically perfect tethered crystal to a low temperature pinned phase is washed out in the presence of thermally excited dislocation pairs. Analogous behavior is encountered in the random field XY model [3]. An extension to vector displacement fields has been studied by Giamarchi and LeDoussal [9].

The hexatic liquid crystalline phase of the *untethered* membrane above T_M [see Fig. 2(a)] displays similar behavior when subjected to a component of the random substrate disorder which couples directly to the bond angle field. The analogy with the random field XY model [3] becomes a rigorous mapping for annealed hexatic membranes: either disclination unbinding or substrate disorder always destabilize the hexatic line of fixed points, and it is unclear if there is a sharp finite temperature phase transition. Polymerized tethered membranes behave differently, however. Although quenched-in unpaired dislocations destroy translational long range order, they cannot drive the shear modulus to zero. The finite shear modulus makes the bond angle fluctuations ''massive'' [8]. These fluctuations are now stable to weak external disorder.

Quenched topological disorder has recently been studied for ''tethered surfaces'' [10], in which defects are frozen into a two-dimensional network of covalently bonded particles fluctuating in three dimensions. It is of considerable interest to determine what happens when such disordered tethered surfaces are forced to lie flat and brought into contact with a disordered polycrystalline or amorphous substrate. A particularly simple example of such tethered disorder is shown in Fig. 2(b), where a topologically perfect triangular lattice is disrupted by random substitutional disorder. Unfortunately, the method used in this paper cannot be directly applied to such systems [11]. Tethered substitutional disorder invalidates a straightforward analogy with random field models (see Sec. II). Cule and Hwa studied this problem in one dimension, and concluded that a new, strongly pinned glassy phase arises, characterized by exponents in the ''random manifold'' universality class [12]. Similar results may apply to two-dimensional tethered networks with quenched-in vacancies, interstitials, dislocations, or disclinations, as well as random substitutional disorder [12].

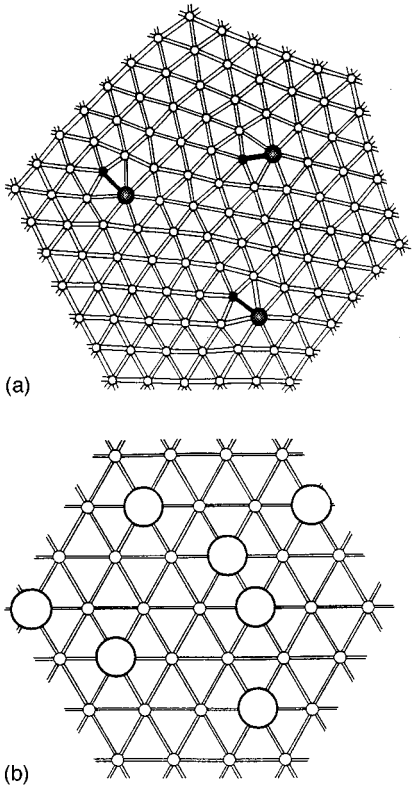

FIG. 2. (a) Annealed dislocation disorder embedded in an otherwise sixfold-coordinated membrane. Heavy lines join the 5- and 7-coordinated sites at the cores of the dislocations. The disordered substrate potential is not shown. (b) Random substitutional disorder in a polymerized membrane which preserves the sixfold coordination of a perfect lattice. The disordered substrate potential which acts on this lattice is not shown.

A theory of *three*-dimensional tethered networks with both quenched random internal defects *and* a quenched random external potential would have interesting implications for the tangled arrays of vortex lines which may arise when bulk type II superconductors are subjected to strong external magnetic fields. If melted flux liquids are cooled rapidly, barriers to flux cutting [13] may become sufficiently large that the vortex lines freeze at low temperatures into a nonequilibrium directed ''polymer glass'' [14]. The usual triangular Abrikosov flux lattice would then be disrupted by a quenched array of dislocation and disclination lines of arbitrarily large size. The resulting vortex array could have a shear modulus over a wide range of experimental time scales because of entanglement constraints, and would be subject to point pinning by imperfections in the underlying host superconducting material.

This paper is organized as follows. In Sec. II, we present the theory of ideal (topologically perfect) two-dimensional crystals subject to external point disorder. Effects of annealed dislocations are discussed in Sec. III, and some concluding remarks are presented in Sec. IV. Some of the effects of quenched substitutional disorder are discussed in Appendix A. Technical details of the derivation of the renormaliza-

tion group recursion relations used in Sec. II are contained in Appendix B. Appendix C derives the exponent z for a relaxational model of tethered crystalline membrane dynamics. An Ornstein-Zernicke description of the hexatic phase is derived in Appendix D.

II. PINNING OF IDEAL CRYSTALS

Consider a two-dimensional Bravais lattice $\vec{R}_{mn}=m\vec{a}+n\vec{b}$, and denote by $\vec{u}(m,n)$ the displacement from the equilibrium position $\vec{R}_{mn}$. We begin by restricting our analysis to an ideal lattice of identical particles, where the displacements are single-valued functions of position. Thus we exclude for the moment the possibility of topological defects. The strains associated with random substitutional disorder will be discussed later in this section. The energy of an ideal crystal undergoing a small deformation can be expressed, using continuum elasticity theory, by the harmonic Hamiltonian

$$H_0=\tfrac{1}{2}\int d^2r(\lambda u_{ii}^2+2\mu u_{ij}^2), \tag{2.1}$$

where λ and μ are Lamé coefficients, and the strain tensor is defined as

$$u_{ij}(\vec{r})=\tfrac{1}{2}(\partial_i u_j+\partial_j u_i). \tag{2.2}$$

The only regular lattice in two dimensions with sufficient symmetry to be described by the *isotropic* elastic theory (2.1) is a triangular array [15]. In this case, it is convenient to take

$$\vec{a}=a_0(1,0), \quad \vec{b}=a_0\left(\frac{1}{2},\frac{\sqrt{3}}{2}\right), \tag{2.3}$$

where a_0 is the lattice constant.

If the lattice is subjected to an external pinning potential, the total pinning energy is given by $U_{\rm pin}=\Sigma_{mn}V[\vec{R}_{mn}+\vec{u}(m,n)]$. With the aid of Poisson's summation formula, we write

$$\begin{aligned}U_{\rm pin}&=\int d^2rV(r)\sum_{mn}\delta^2[\vec{r}-\vec{R}_{mn}-\vec{u}(m,n)]\\&=\int d^2rV(r)\int d\sigma_1\int d\sigma_2\delta^2[\vec{r}-\sigma_1\vec{a}-\sigma_2\vec{b}\\&\quad-\vec{u}(\sigma_1,\sigma_2)]\sum_{pq}e^{2\pi i(p\sigma_1+q\sigma_2)},\end{aligned} \tag{2.4}$$

where (m,n) and (p,q) are pairs of integers. Next we change integration variables from σ_1,σ_2 to $\vec{r}=(x,y)=\sigma_1\vec{a}+\sigma_2\vec{b}+\vec{u}(\sigma_1,\sigma_2)$. The Jacobian of this tranformation is

$$\frac{\partial\sigma_1}{\partial x}\frac{\partial\sigma_2}{\partial y}-\frac{\partial\sigma_1}{\partial y}\frac{\partial\sigma_2}{\partial x}\simeq\frac{1}{|\vec{a}\times\vec{b}|}(1-\vec{\nabla}\cdot\vec{u}). \tag{2.5}$$

The δ function in Eq. (2.4) fixes the values of σ_1 and σ_2 to be the root of

$$\sigma_1\vec{a}+\sigma_2\vec{b}+\vec{u}(\sigma_1,\sigma_2)=\vec{r}, \tag{2.6}$$

which can be expanded as a power series in the small displacement $\vec{u}$. Upon noting that the zeroth order term is

$$\sigma_1^0=\frac{(\vec{r}\times\vec{b})\cdot\hat{\mathbf{z}}}{|\vec{a}\times\vec{b}|}, \quad \sigma_2^0=-\frac{(\vec{r}\times\vec{a})\cdot\hat{\mathbf{z}}}{|\vec{a}\times\vec{b}|} \tag{2.7}$$

and using the δ function to eliminate the integrals over σ_1 and σ_2, we can write the total pinning energy as

$$U_{\rm pin}\approx\int d^2rV(r)\frac{1}{|\vec{a}\times\vec{b}|}(1-\vec{\nabla}\cdot\vec{u})\sum_{mn}e^{i\vec{G}_{mn}\cdot[\vec{r}-\vec{u}(\vec{r})]}, \tag{2.8}$$

where $\{\vec{G}_{mn}\}$ are reciprocal lattice vectors. The total Hamiltonian of the system is obtained by adding the Hamiltonian of an ideal two-dimensional crystal to the pinning energy. We study the effect of a random distribution of weak pinning potentials, with mean and variance defined by

$$\overline{V(\vec{r})}=0, \quad \overline{V(\vec{r})V(\vec{r}')}=\Delta\delta^2(\vec{r}-\vec{r}'). \tag{2.9}$$

If we restrict our attention to the seven smallest reciprocal lattice vectors (including $\vec{G}_{mn}=0$) in the summation of Eq. (2.8), then the total Hamiltonian which comprises our model may be approximated (up to an additive constant) by

$$\begin{aligned}\mathcal{H}=\frac{1}{2}\int d^2r\Bigg(&\lambda u_{ii}^2+2\mu u_{ij}^2-w(\vec{r})u_{ii}\\&+\sum_{l=1}^{3}V_{G_l}(\vec{r})e^{-i\vec{G}_l\cdot\vec{u}(\vec{r})}\Bigg),\end{aligned} \tag{2.10}$$

where the $\vec{G}_l$, $l=1$, 2, and 3, are three reciprocal lattice vectors inclined at 120° angles to each other in the innermost ring,

$$w(\vec{r})=\frac{V(\vec{r})}{|\vec{a}\times\vec{b}|}, \tag{2.11}$$

and $V_{\vec{G}}(\vec{r})$ is a local Fourier component of the random potential,

$$V_{\vec{G}}(\vec{r})=\frac{1}{\Delta\Omega}\int d^2r'e^{i\vec{G}\cdot\vec{r}'}\frac{V(\vec{r}')}{|\vec{a}\times\vec{b}|}. \tag{2.12}$$

The integration is carried out over an area $\Delta\Omega$, centered on $\vec{r}$, large compared to the lattice spacing but small compared to the sample dimensions. We have neglected terms of the form $\vec{\nabla}\cdot\vec{u}\,\exp(i\vec{G}_l\cdot[\vec{r}-\vec{u}(\vec{r})])$, which are irrelevant variables on the surface of fixed points we discuss below. In Appendix A, we show that random substitutional disorder contributes to $w(\vec{r})$ and leads as well to a random term of the form $-\frac{1}{2}\int d^2r\, w_{ij}(\vec{r})u_{ij}(\vec{r})$. A two-dimensional bead and spring model [1] with random spring lengths contains similar contributions. Quenched substitutional disorder has important additional effects, however. Internal disorder in the particle

sizes or bond lengths violates the *discrete* translational invariance of the Hamiltonian (2.10) under $\vec{u}(\vec{r}) \to \vec{u}(\vec{r}) + \vec{R}_{mn}$. Cule and Hwa argued that this symmetry breaking leads to an effective ''random manifold'' potential which depends in a complicated way on *both* $\vec{r}$ and $\vec{u}(\vec{r})$, and causes an instability to a more strongly pinned glassy phase than the one studied here [12].

For tethered networks of *identical* particles, we expect that pinning effects due to the random phases and amplitudes embodied in $\{V_{G_l}\}$ will be important below some critical temperature, and that the properties of the system in the vicinity of this temperature will be perturbatively accessible by renormalization group methods. The starting point of the renormalization program is perturbation theory. Computation of the disorder-averaged observables of interest, such as the free energy or the two-point functions, requires expanding the logarithm of the partition function $\mathcal{Z}$ in powers of the weak pinning potential and averaging term by term. Such averages are conveniently handled by the replica trick, which involves first calculating $\mathcal{Z}^n = 1 + n \ln \mathcal{Z} + O(n^2)$ and eventually taking the limit $n \to 0$. The disorder average of $\mathcal{Z}^n$ leads to

$$\overline{\mathcal{Z}^n} = \int \mathcal{D}\vec{u}_1 \cdots \mathcal{D}\vec{u}_n e^{-\mathcal{H}_n^0/T - \mathcal{H}_n^I/T}, \tag{2.13}$$

where the harmonic term is

$$\frac{\mathcal{H}_n^0}{T} = \frac{1}{2T} \sum_{\alpha\beta}^{n} \int \frac{d^2k}{(2\pi)^2} u_{i\alpha}(-\vec{k}) k^2 \{[\mu P_{ij}^T + (2\mu + \lambda) P_{ij}^L] \delta_{\alpha\beta} - B P_{ij}^T - A P_{ij}^L\} u_{j\beta}(\vec{k}), \tag{2.14}$$

and the interaction term is

$$\frac{\mathcal{H}_n^I}{T} = -g \sum_{l=1}^{3} \int d^2r \sum_{\alpha\beta}^{n} \cos(\vec{G}_l \cdot [\vec{u}_\alpha(\vec{r}) - \vec{u}_\beta(\vec{r})]). \tag{2.15}$$

Greek indices label different replicas, while latin subscripts $(i,j = 1,2)$ are used for the components of the displacement vector $\vec{u}$. Summation over repeated indices i and j is understood. The vectors $\vec{G}_l$ are the smallest nonzero vectors in the reciprocal lattice. For a triangular lattice of spacing a_0, $l = 1,2,3$ and $|G_l|^2 = 16\pi^2/3a_0^2$. Effects due to reciprocal lattice vectors of larger norm are irrelevant.

The structure of the replicated Hamiltonian is quite simple. The harmonic part contains a term diagonal in the replica indices. This is simply the replicated Hamiltonian of an ideal two-dimensional crystal in Fourier space, where P_{ij}^L and P_{ij}^T are longitudinal and transverse projectors, respectively. In addition, transverse and longitudinal terms are considered, which are constant in replica space. The tranverse term, while not present initially, is generated by renormalization. Its coefficient B can be set to zero initially. The cosine term arises as a consequence of the discrete nature of the lattice. Its amplitude is related to the correlation function of the randomness by

$$g = \frac{\Delta}{T^2 \Omega^2}, \tag{2.16}$$

where $\Omega = |\vec{a} \times \vec{b}|$ is the area of the unit cell.

The use of replicas brings out an important property of the model. Note that the interaction term involves only differences of fields with different replica indices. Hence the ''center of mass,'' in replica space, of the fields $\vec{u}_\alpha$,

$$\vec{\Psi} \equiv n^{-1/2} \sum_{\alpha} \vec{u}_\alpha, \tag{2.17}$$

is a free field and does not suffer renormalization. This symmetry implies that $2\mu + \lambda - nA$, $\mu - nB$ do not renormalize, a result valid to all orders in perturbation theory, similar to the invariance under renormalization of the spin wave stiffness in the random-field XY model [16]. As a consequence, the renormalization group flow of the disorder coupling, g, is one dimensional.

Next, consider the connected Green's function

$$\overline{\langle u_i(\vec{r}) u_j(\vec{r}') \rangle_c} = -\frac{\partial^2 \overline{\ln \mathcal{Z}}}{\partial J_i(\vec{r}) \partial J_j(\vec{r}')} = -\frac{1}{n} \frac{\partial^2 \overline{\mathcal{Z}^n[\vec{J}]}}{\partial J_i(\vec{r}) \partial J_j(\vec{r}')}\bigg|_{n=0}, \tag{2.18}$$

obtained from the generating functional

$$\overline{\mathcal{Z}^n[\vec{J}]} = \overline{\mathcal{Z}^n} \left\langle \exp\left(i \int d^2r \, \vec{J}(\vec{r}) \cdot \sum_{\alpha} \vec{u}_\alpha(\vec{r}) \right) \right\rangle_R . \tag{2.19}$$

Hereafter, the notation $\langle \ \rangle_R$ will stand for average with respect to the integrand in Eq. (2.13). Since the source $\vec{J}$ couples only to $\vec{\Psi}$, a free field, this Green's function is the free correlation function, independent of g,

$$\overline{\langle u_i(\vec{r}) u_j(\vec{r}') \rangle_c} = -\delta_{ij} \frac{T}{4\pi\mu} \frac{3\mu + \lambda}{2\mu + \lambda} \ln \frac{|\vec{r} - \vec{r}'|}{a_0} + \text{const}, \quad |\vec{r} - \vec{r}_0| \to \infty, \tag{2.20}$$

where the connected part is $\langle A(x)B(x') \rangle_c = \langle A(x)B(x') \rangle - \langle A(x) \rangle \langle B(x') \rangle$. Thus this connected correlation function is insensitive to the presence of randomness in the system.

The peculiar properties of the glassy phase do appear, however, in the nontrivial behavior of some response functions as well as in the full correlation function $\overline{\langle u_i(\vec{r}) u_j(\vec{r}') \rangle}$, which, according to the analysis above, is a probe of sample-to-sample fluctuations. In the language of replicas, these fluctuations are captured by introducing a replica-dependent source field, $\vec{J}_\alpha(\vec{r})$, and a new generating functional

$$\overline{\mathcal{Z}^n[\{\vec{J}_\alpha\}]} = \overline{\mathcal{Z}^n} \left\langle \exp\left(i \int d^2r \sum_{\alpha} \vec{J}_\alpha(\vec{r}) \cdot \vec{u}_\alpha(\vec{r}) \right) \right\rangle_R . \tag{2.21}$$

Differentiation with respect to $\vec{J}_\alpha$ yields the Green's functions

$$G_{ij\alpha\beta}(\vec{r}-\vec{r}')=\langle u_{i\alpha}(\vec{r})u_{j\beta}(\vec{r}')\rangle_R . \tag{2.22}$$

Provided symmetry under permutation of the replica indices holds, we can write

$$\overline{\langle u_i(\vec{r})u_j(\vec{r}')\rangle_c}=\lim_{n\to 0}[G_{ij11}(\vec{r}-\vec{r}')-G_{ij12}(\vec{r}-\vec{r}')],$$

$$\overline{\langle u_i(\vec{r})u_j(\vec{r}')\rangle}=\lim_{n\to 0}G_{ij11}(\vec{r}-\vec{r}'), \tag{2.23}$$

where the limit $n\to 0$ is here simply a convenient bookkeeping device for doing perturbation theory.

The perturbation series for the disorder-averaged Green's functions diverges in the thermodynamic limit at low temperature. The divergent diagrams are most easily recognized by considering the expansion of the free energy,

$$\overline{(F-F_0)}=-\lim_{n\to 0}\frac{1}{n}(-\langle\mathcal{H}_n^I\rangle_R+\tfrac{1}{2}[\langle(\mathcal{H}_n^I)^2\rangle_R - \langle(\mathcal{H}_n^I)\rangle_R^2]+\cdots). \tag{2.24}$$

Upon defining a reduced temperature

$$\tau\equiv 1-\frac{T}{T_g}=1-\frac{T|G|^2}{8\pi\mu}\frac{3\mu+\lambda}{2\mu+\lambda}, \tag{2.25}$$

one finds, up to regular terms, in order g,

$$-\frac{\langle\mathcal{H}_n^I\rangle_R}{T}\sim gca^2n(n-1)3\pi(L/a\sqrt{c})^{2\tau}, \tag{2.26}$$

and, in order (g^2),

$$\frac{1}{2T^2}\langle(\mathcal{H}_n^I)^2\rangle_R\sim -g^2c^2a^4n(n-1)[I_0(\psi)+(n-2)I_0(\psi/2)] \times 3\pi^2\left(\frac{L}{a\sqrt{c}}\right)^{2\tau}\frac{2}{2\tau}[(L/a\sqrt{c})^{2\tau}-1]. \tag{2.27}$$

Infrared and ultraviolet cutoffs L and a, respectively, have been introduced; $c=\frac{1}{4}e^{2E}\approx 0.79$, where E is Euler's constant; I_0 is a modified Bessel function, and

$$\psi\equiv\frac{T|G|^2(\mu+\lambda)}{4\pi\mu(2\mu+\lambda)}. \tag{2.28}$$

The details of the calculation can be found in Appendix B.

The divergences can be removed order by order in a double expansion in powers of g and τ. The parameters of the renormalized theory transform, under rescaling of length by e^l, according to the following equations:

$$\frac{d\lambda}{dl}=0,$$

$$\frac{d\mu}{dl}=0,$$

$$\frac{d\tilde{g}}{dl}=2\tau\tilde{g}-\frac{2}{3}\tilde{g}^2[2I_0(\psi/2)-I_0(\psi)], \tag{2.29}$$

$$\frac{dA}{dl}=\tilde{g}^2\tfrac{4}{3}\mu\frac{2\mu+\lambda}{3\mu+\lambda}[I_0(\psi)-\tfrac{1}{2}I_1(\psi)],$$

$$\frac{dB}{dl}=\tilde{g}^2\tfrac{4}{3}\mu\frac{2\mu+\lambda}{3\mu+\lambda}[I_0(\psi)+\tfrac{1}{2}I_1(\psi)],$$

where $\tilde{g}\equiv 3\pi gca^2(L/a\sqrt{c})^{2\tau}$. The flow of the disorder coupling to zero for $\tau<0$, i.e., for $T>T_g$, means that the discreteness of the lattice is irrelevant in the high temperature phase. Thus the correlation functions in this phase are similar to the Gaussian model of Ref. [17]. In particular,

$$\overline{\langle u_i(\vec{r})u_i(0)\rangle}\sim -\eta\ln r, \tag{2.30}$$

where

$$\eta=|\vec{G}|^2\left(\frac{T}{4\pi\mu}\frac{3\mu+\lambda}{2\mu+\lambda}+\frac{\Delta}{4\pi(2\mu+\lambda)^2} + \frac{A}{4\pi(2\mu+\lambda)^2}+\frac{B}{4\pi\mu^2}\right). \tag{2.31}$$

Below T_g, on the other hand, the disorder coupling flows toward a finite fixed point value of $\tilde{g}^*=3\tau/[2I_0(\psi/2)-I_0(\psi)]$. The runaway flows of A and B cause the correlation function in Eq. (2.30) to grow as $\ln^2 r$, a behavior which was termed ''super-roughening'' in the context of scalar models of surface growth [18].

The change in equilibrium correlation functions from ''rough'' $\ln r$ growth to ''super-rough'' $\ln^2 r$ growth is a characteristic of the low temperature glassy phase [3,18]. Another distinctive property of the glassy phase is the nontrivial near-equilibrium dynamics. The dissipative dynamics of the system embodied in the Langevin equation

$$\gamma\partial_t\vec{u}=-\frac{\delta H}{\delta\vec{u}}+\vec{\zeta}, \tag{2.32}$$

with $\vec{\zeta}$ a thermal noise, can also be studied by dynamical renormalization group methods [19]. The detailed treatment of this model is described in Appendix C. Regularization of the perturbative expansion of the dynamic response leads to a renormalized friction coefficient γ, from which the dynamic exponent can be extracted

$$z=2,\quad T>T_g,$$

$$z=2+\frac{24}{\sqrt{c}}\frac{2\mu+\lambda}{3\mu+\lambda}\left(\frac{\mu}{2\mu+\lambda}\right)^{\mu/(3\mu+\lambda)}\frac{\tau}{[2I_0(\psi/2)-I_0(\psi)]},$$

$$T<T_g, \tag{2.33}$$

where $c=\frac{1}{4}e^{2E}\approx 0.79$ is the same function of Euler's constant as appears in the static calculation, and ψ was defined in Eq. (2.28).

III. EXTERNAL DISORDER AND TOPOLOGICAL DEFECTS

The foregoing discussion assumed the fixed topology of an ideal lattice. Spontaneous nucleation of topological defects, which occurs above the melting temperature

$$T_M=\frac{\mu}{4\pi}\frac{\mu+\lambda}{2\mu+\lambda}a^2, \tag{3.1}$$

destroys translational long range order [8]. The ratio of the glass temperature to the melting temperature is always greater than 1 (in fact, $T_g/T_M \geq 6$ for all elastic constant values in the physically relevant range $\mu>0$, $\mu+\lambda>0$), so that dislocations are expected to be a strongly relevant perturbation at T_g. Thus *either* the random substrate potential or thermally excited dislocation pairs always destabilize the harmonic Hamiltonian, and the transition of Sec. II does not occur in the presence of annealed topological defects.

Although annealed dislocations destroy translational long range order, the resulting hexatic phase does possess (algebraic) long range order in the bond angle. A harmonic Hamiltonian for the hexatic phase can be obtained in the Ornstein-Zernicke approximation, valid at long wavelength. The details of the derivation are presented in Appendix D. We can consider the stability of the long wavelength Hamiltonian, Eq. (D14), to an external random potential coupled to the bond angle. An experimental realization of this system is provided by a hexatic liquid crystalline film adsorbed onto a polycrystalline substrate, that is, a substrate whose randomly varying crystallographic axes locally bias the orientation of the bonds in the film. The total Hamiltonian becomes precisely that of a random field XY model, which was studied by Cardy and Ostlund [3]. Similar to the case of *untethered* crystalline films discussed above, it follows from Ref. [3] that the harmonic Hamiltonian (D14) is always destabilized either by the external disorder or by thermally excited *disclinations*. There is an important difference between crystalline and hexatic membranes, however. In the case of a crystalline membrane, the ideal topology can be fixed by polymerization, and the fixed line discovered in Sec. II should be experimentally accessible. In contrast, it is impossible to prevent disclinations from destabilizing the vortex glass fixed line in a hexatic film, except by quenching the topology of the film. However, in this case Eq. (D14) reveals, upon treating the singular density and bond angle fluctuations $\delta\rho_s$ and $\delta\theta_s$ as quenched variables, that this quenched hexatic phase has a finite shear modulus, rendering the bond fluctuations massive. Because of the finite shear modulus, the bond angle excitations are stable to weak disorder. Whether a tethered hexatic (or liquid) film is unstable to a ''random manifold'' glassy state [12] is an interesting subject for future investigation.

IV. DISCUSSION AND CONCLUSIONS

In this paper, we studied the physics of 2+0-dimensional arrays of identical particles in an external random potential, using a vector extension of the 1+1-dimensional random phase model. The predictions for vector models without topological defects are qualitatively similar to the scalar model: the discreteness of the vortex array coherently enhances the Fourier components of the external disorder which are commensurate with the lattice, leading to a glassy phase at low temperature. This phase is characterized by a nonlinear response to an external driving force, as well as by static correlations which diverge more strongly than a simple logarithm. Quantitative expressions for the static and dynamic exponents near the transition were computed within a perturbative renormalization group scheme.

The physics changes completely, if annealed topological defects are allowed in the two-dimensional lattice. The possibility of important topological defects constitutes the principal difference between the 2+0- and the 1+1-dimensional models of vortex arrays. Both annealed and quenched dislocations have been considered, the most interesting case being provided by quenched dislocations. The nonvanishing shear modulus of a membrane with quenched-in dislocations prevents the bond angle from following the random bias of an external polycrystalline substrate, so that the bond angle order parameter in quenched hexatics is stable to weak disorder of this type [20].

Our study is relevant to several other situations besides the pinning of vortex arrays in type II superconductors. Systems of current experimental interest were mentioned in Sec. I. Here we would like to comment on possible applications to tribology, the study of friction and lubrication. We are interested in the behavior of two surfaces brought in contact and rubbed against each other in the presence of an intermediate thin layer of lubricant. This boundary layer is often modeled as a two-dimensional, incommensurate crystalline overlayer [21]. Our work may be useful in generating more realistic descriptions which allow for (a) surface imperfections, acting as pinning centers on the lubricant overlayer; and (b) changes in topology of the overlayer, especially excitation of dislocations, which must surely be important at finite temperature and/or under finite stresses. We leave the pursuit of this interesting topic to future work.

Noted added: After this paper was submitted, we received an interesting preprint by D. Carpentier and P. Le Doussal (cond-mat/9611168) which reaches similar conclusions using a different renormalization group method. Comparison with their results enabled us to uncover an error in the first version of our paper, which, although it did not affect our basic conclusions, changes the coefficients in our recursion relations. Once the error is corrected, results obtained by the different methods agree. We are grateful to P. Le Doussal for bringing this discrepancy to our attention.

ACKNOWLEDGMENTS

We acknowledge helpful discussions with T. Hwa. This work was supported by the National Science Foundation, at Harvard University principally through the Harvard Materials Research and Engineering Center through Grant No. DMR91-06237 and through Grant No. DMR91-15491, and at UC Berkeley through Grant No. CHE 9508336. Support by the Office of Naval Research under Grant No. N00014-92-J-1361 at UC Berkeley is also gratefully acknowledged.

APPENDIX A

Effects due to a disordered *substrate* were incorporated into isotropic two-dimensional elasticity theory in Sec. II. In this appendix, we discuss effects on the elastic properties due to random substitutional disorder *in the membrane*, as exemplified by the large impurity atoms displayed in Fig. 2(b). We do *not* discuss the important interplay between random substitutional disorder and the disorder substrate potential [12]. A distribution of impurity atoms with sizes different from the average leads to random strains. *Annealed* defects of this kind can be integrated out and simply alter the elastic constants μ and λ. As we shall see, the strains in the quenched case contribute to the coefficients A and B displayed in the replicated Hamiltonian, Eq. (2.14). Quenched random vacancy or interstitial defects as well as tightly bound dislocations pairs or triplets would affect A and B similarly. We work with a continuum model studied already in the context of random tethered surfaces fluctuating in three dimensions [10]. The only change required is neglect of displacements normal to the average plane of the membrane. These phonon modes become massive due to the interaction with the substrate and can be integrated out without affecting our basic results.

We assume a topolgically perfect lattice and replace $\vec{R}_{mn}$ by a coarse-grained function $\vec{R}(\vec{r})$ which gives the lattice displacement $\vec{R}$ as a function of the reference position $\vec{r}$. We use a generalization of Eq. (2.1),

$$H=\tfrac{1}{2}\int d^2r(\lambda u_{ii}^2+2\mu u_{ij}^2), \tag{A1}$$

where the strain matrix is now given by [10]

$$u_{ij}=\tfrac{1}{2}(\partial_i\vec{R}\cdot\partial_j\vec{R}-\partial_i\vec{R}^0\cdot\partial_j\vec{R}^0). \tag{A2}$$

Here $\vec{R}^0(\vec{r})$ is a preferred lattice distortion which minimizes the energy in the absence of thermal fluctuations. In the absence of defects, $\partial_i\vec{R}^0\cdot\partial_j\vec{R}^0=\delta_{ij}$. Localized defects like substitutional disorder, vacancies, interstitials, etc., lead to deviations which we parametrize by

$$\partial_i\vec{R}^0\cdot\partial_j\vec{R}^0=\delta_{ij}+c_{ij}(\vec{r}). \tag{A3}$$

If we assume an uncorrelated Gaussian disorder, the probability distribution of the tensor $c_{ij}(\vec{r})$ takes the form [10]

$$\mathcal{P}_r[c_{ij}(\vec{r})]\propto\exp\left(-\frac{1}{2\sigma_1}\int d^2r c_{ii}^2-\frac{1}{2\sigma_2}\int d^2r\ c_{ij}^2\right). \tag{A4}$$

We now set $\vec{R}(\vec{r})=\vec{r}+\vec{u}(\vec{r})$, so that

$$\partial_i\vec{R}\cdot\partial_j\vec{R}=\delta_{ij}+\tfrac{1}{2}(\partial_iu_j+\partial_ju_i)+\tfrac{1}{2}\partial_i\vec{u}\cdot\partial_j\vec{u}\approx\delta_{ij}+u_{ij}. \tag{A5}$$

Hamiltonian (A1) then takes the form

$$H=\text{const}+\tfrac{1}{2}\int d^2r[\lambda u_{ii}^2+2\mu u_{ij}^2-\lambda c_{ii}(\vec{r})u_{jj}(\vec{r})-2\mu c_{ij}(\vec{r})u_{ij}]. \tag{A6}$$

The term proportional to u_{ii} represents random dilations or contractions due to isolated impurities in positions of high symmetry, while the more complicated tensorial coupling describes more anisotropic defect configurations. Upon replicating this Hamiltonian and tracing out the Gaussian disorder, we obtain contributions to the coefficients A and B in Eq. (2.14).

APPENDIX B

This appendix details the calculations leading to the flow equations for g, A, and B. We begin by evaluating the right hand side of Eq. (2.24) term by term. To order g,

$$\begin{aligned}\left\langle\frac{\mathcal{H}_n^I}{T}\right\rangle&=-g\sum_{l=1}^{3}\int d^2r\sum_{\alpha\beta}^{n}\langle\exp\{i\vec{G}_l\cdot[\vec{u}_\alpha(\vec{r})-\vec{u}_\beta(\vec{r})]\}\rangle\\&=-g\sum_{l=1}^{3}\int d^2r\sum_{\alpha\beta}^{n}\exp\left[-T\int\frac{d^2k}{(2\pi)^2}\frac{1}{k^2}G_i^l\right.\\&\quad\left.\times\left(\frac{1}{\mu}P_{ij}^T+\frac{1}{2\mu+\lambda}P_{ij}^L\right)G_j^l\right].\end{aligned} \tag{B1}$$

Before proceeding with the calculation, we must introduce cutoffs to deal with infrared and ultraviolet singularities arising from integrals of the type

$$\int\frac{d^2k}{(2\pi)^2}G_i^l\frac{e^{i\vec{k}\cdot\vec{r}}}{k^2}P_{ij}^{T,L}G_j^l. \tag{B2}$$

A long wavelength cutoff L is introduced to eliminate infrared divergences. Its effect amounts to shifting $1/k^2\to1/(k^2+L^{-2})$. The limit $L\to\infty$ can be taken safely at the end of the calculations. The ultraviolet divergences are removed in coordinate space by the simple shift $r\to\sqrt{r^2+a^2}$, where a is a short wavelength cutoff of order the lattice constant. Note the short distance limit

$$\begin{aligned}\int\frac{d^2k}{(2\pi)^2}\frac{e^{i\vec{k}\cdot\vec{s}}}{k^2+L^{-2}}\bigg|_{s^2=r^2+a^2}&=\frac{1}{2\pi}K_0\left(\sqrt{\frac{r^2+a^2}{L}}\right)\\&\to-\frac{1}{4\pi}\log c\frac{(r^2+a^2)}{L^2},\end{aligned}\qquad\frac{r}{L}\ll1. \tag{B3}$$

Here, K_0 is a modified Bessel function, and $c=(1/4)e^{2\gamma}$, where γ is Euler's constant. Thus, the asymptotic behavior of the integrals in Eq. (B2) is readily evaluated

$$\begin{aligned}\int\frac{d^2k}{(2\pi)^2}G_i^l\frac{e^{i\vec{k}\cdot\vec{r}}}{k^2}P_{ij}^{T,L}G_j^l&\to-\frac{|G|^2}{8\pi}\ln\frac{c(r^2+a^2)}{L^2}\\&\pm\left(\frac{(\vec{G}\cdot\vec{r})^2}{4\pi r^2}-\frac{|G|^2}{8\pi}\right).\end{aligned} \tag{B4}$$

Upon substituting into Eq. (B1), and recalling Eq. (2.25), which defines the reduced temperature $\tau\equiv1-(T/T_g)=1-(T|G|^2/8\pi\mu)(3\mu+\lambda/2\mu+\lambda)$, we obtain Eq. (2.26).

Next, in order g^2, one has

$$\left\langle \left(\frac{\mathcal{H}_n^I}{T} \right)^2 \right\rangle = g^2 \sum_{l=1}^{3} \sum_{l'=1}^{3} \sum_{\alpha\beta}^{n} \sum_{\alpha'\beta'}^{n} \int d^2r \int d^2r' \langle \exp\{i\vec{G}_l \cdot (\vec{u}_\alpha(\vec{r}) - \vec{u}_\beta(\vec{r})]\} \exp\{i\vec{G}_{l'} \cdot [\vec{u}'_\alpha(\vec{r}') - \vec{u}'_\beta(\vec{r}')]\} \rangle$$

$$= g^2 \sum_{l=1}^{3} \sum_{l'=1}^{3} \sum_{\alpha\beta}^{n} \sum_{\alpha'\beta'}^{n} \left(\frac{\tilde{a}}{L} \right)^{(4-4\tau)} \int d^2r \int d^2r' \exp\left(-TQ_{\alpha\beta}^{\alpha'\beta'} \frac{\vec{G}_l \cdot \vec{G}_{l'}}{8\pi\mu} \frac{3\mu+\lambda}{2\mu+\lambda} \ln \frac{c(|\vec{r}-\vec{r}'|^2 + a^2)}{L^2} \right)$$

$$\times \exp\left[-TQ_{\alpha\beta}^{\alpha'\beta'} \frac{(\mu+\lambda)}{4\pi\mu(2\mu+\lambda)} \left(\vec{G}_l \cdot (\hat{r}-\hat{r}') \vec{G}_{l'} \cdot (\hat{r}-\hat{r}') - \tfrac{1}{2} \right) \right], \tag{B5}$$

where $Q_{\alpha\beta}^{\alpha'\beta'} = \delta_{\alpha\alpha'} + \delta_{\beta\beta'} - \delta_{\alpha\beta'} - \delta_{\alpha'\beta}$, and use has been made of Eq. (B3) in anticipation of the thermodynamic limit. Hereafter, $\tilde{a} \equiv \sqrt{c}a$ and $\psi \equiv [T|G|^2(\mu+\lambda)]/[4\pi\mu(2\mu+\lambda)]$.

Logarithmic divergencies appear, at the critical temperature ($\tau = 0$), when $\vec{G}_l \cdot \vec{G}_{l'} Q_{\alpha\beta}^{\alpha'\beta'}/|G|^2 = 1$. The logarithmically divergent terms contribute to the multiplicative renormalization of the coupling g, while all other terms can be absorbed into an additive constant. (Had we chosen to renormalize the self energy, the need of an additive renormalization would not have arisen, but the calculations would have been considerably more involved.) To proceed, we first fix l, α, and β, which can be done in $3n(n-1)$ independent ways. Then, logarithmic contributions arise either for $l' = l$, $Q_{\alpha\beta}^{\alpha'\beta'} = 1$, or for $l' \neq l$, $Q_{\alpha\beta}^{\alpha'\beta'} = -2$. The respective combinatorial weights are $2(n-2)$ and 2. Carrying out the remaining integrals leads to Eq. (2.27).

We now compute the flow of the coupling constants A, B under renormalization group transformations. Because the self-energy is momentum independent in the first order of perturbation theory, the lowest order contribution to the perturbative renormalization of A, B arises in $O(g^2)$. The free propagator in momentum space, obtained from Eq. (2.14), can be written as the sum of two terms:

$$G_{ij\alpha\beta}^0(k) = M_{ij}(k)\delta_{\alpha\beta} + N_{ij}(k),$$

$$M_{ij}(k) = \frac{1}{k^2} \left(\frac{1}{\mu} P_{ij}^T + \frac{1}{2\mu+\lambda} P_{ij}^L \right), \tag{B6}$$

$$N_{ij}(k) = \frac{1}{k^2} \frac{B}{\mu(\mu - nB)} P_{ij}^T + \frac{1}{k^2} \frac{A}{(2\mu+\lambda)(2\mu+\lambda-nA)} P_{ij}^L .$$

The perturbative expansion of the generating functional Eq. (2.21) through second order reads as

$$\overline{\mathcal{Z}^n[\{\vec{J}_\alpha\}]} = \exp\left(-\frac{T}{2} \int \frac{d^2k}{(2\pi)^2} \sum_\alpha \sum_{ij} J_{i\alpha}(\vec{k}) M_{ij}(k) J_{j\alpha}(-\vec{k}) + \sum_{\alpha\beta} J_{i\alpha}(\vec{k}) N_{ij}(k) J_{j\beta}(-\vec{k}) \right)$$

$$\times \left(1 + g\mathcal{F}_1(J) + \frac{g^2}{2} \mathcal{F}_2(J) + \cdots \right), \tag{B7}$$

where

$$\mathcal{F}_2(J) = \sum_{ll'} \sum_{\alpha\beta} \sum_{\alpha'\beta'} \int d^2r \int d^2r' \left(\frac{\tilde{a}}{L} \right)^{(4-4\tau)} \exp\left(-TQ_{\alpha\beta}^{\alpha'\beta'} \sum_{ij} G_i^l M_{ij}(\vec{r}-\vec{r}') G_j^{l'} \right) \exp\left[-T \int \frac{d^2k}{(2\pi)^2} \right.$$

$$\left. \times \left(\sum_{ij} G_i^l M_{ij}(k) [J_{j\alpha}(\vec{k}) - J_{j\beta}(\vec{k})] e^{-i\vec{k}\cdot\vec{r}} + \sum_{ij} G_i^{l'} M_{ij}(k) (J_{j\alpha'}(\vec{k}) - J_{j\beta'}(\vec{k})) e^{-i\vec{k}\cdot\vec{r}'} \right) \right]. \tag{B8}$$

Thus the renormalized propagator $N_{ij}^R(k)$ can be calculated perturbatively as

$$-TN_{ij}^R(k)\delta(\vec{k}+\vec{k}') = -TN_{ij}(k)\delta(\vec{k}+\vec{k}') + \frac{(2\pi)^2 g^2}{2} \left. \frac{\delta^2 \mathcal{F}_2(J)}{\delta J_{i\lambda}(\vec{k}) \delta J_{j\mu}(\vec{k}')} \right|_{J=0} + \cdots, \tag{B9}$$

with

$$\left.\frac{\delta^2\mathcal{F}_2(J)}{\delta J_{i\lambda}(\vec{k})\,\delta J_{j\mu}(\vec{k}')}\right|_0 = \sum_{ll'}\sum_{\alpha\beta}\sum_{\alpha'\beta'}\int d^2r\int d^2r'\left(\frac{\tilde{a}}{L}\right)^{(4-4\tau)}\exp\left(-TQ^{\alpha'\beta'}_{\alpha\beta}\sum_{i'j'}G^{l}_{i'}M_{i'j'}(\vec{r}-\vec{r}')G^{l'}_{j'}\right)\frac{T^2}{(2\pi)^4}\sum_{i'j'}$$
$$\times[G^{l}_{i'}M_{i'i}(k)(\delta_{\alpha\lambda}-\delta_{\beta\lambda})e^{-i\vec{k}\cdot\vec{r}}+G^{l'}_{i'}M_{i'i}(k)(\delta_{\alpha'\lambda}-\delta_{\beta'\lambda})e^{-i\vec{k}\cdot\vec{r}'}][G^{l}_{j'}M_{j'j}(k')(\delta_{\alpha\mu}-\delta_{\beta\mu})e^{-i\vec{k}'\cdot\vec{r}}$$
$$+G^{l'}_{j'}M_{j'j}(k')(\delta_{\alpha'\mu}-\delta_{\beta'\mu})e^{-i\vec{k}'\cdot\vec{r}'}]. \tag{B10}$$

Contributions behaving as $1/k^2$ for small k arise from

$$\sum_{ll'}\sum_{\alpha\beta}\sum_{\alpha'\beta'}\int d^2r\int d^2r'\left(\frac{\tilde{a}}{L}\right)^{(4-4\tau)}\exp\left(-TQ^{\alpha'\beta'}_{\alpha\beta}\sum_{ij}G^{l}_{i}M_{ij}(\vec{r}-\vec{r}')G^{l'}_{j}\right)\frac{T^2}{(2\pi)^4}\sum_{mm'}[G^{l}_{m}M_{mi}(k)(\delta_{\alpha\lambda}-\delta_{\beta\lambda})$$
$$\times e^{-i\vec{k}\cdot\vec{r}}G^{l'}_{m'}M_{m'j}(k')(\delta_{\alpha'\mu}-\delta_{\beta'\mu})e^{-i\vec{k}'\cdot\vec{r}'}+G^{l'}_{m}M_{mi}(k)(\delta_{\alpha'\lambda}-\delta_{\beta'\lambda})e^{-i\vec{k}\cdot\vec{r}'}G^{l}_{m'}M_{m'j}(k')(\delta_{\alpha\mu}-\delta_{\beta\mu})e^{-i\vec{k}'\cdot\vec{r}}]$$
$$=\delta(\vec{k}+\vec{k}')\sum_{ll'}\sum_{\alpha\beta}\sum_{\alpha'\beta'}\int d^2s\left(\frac{\tilde{a}}{L}\right)^{(4-4\tau)}\exp\left(-TQ^{\alpha'\beta'}_{\alpha\beta}\sum_{ij}G^{l}_{i}M_{ij}(s)G^{l'}_{j}\right)\frac{-T^2}{(2\pi)^2}(\vec{k}\cdot\vec{s})^2\sum_{mm'}G^{l}_{m}G^{l'}_{m'}M_{mi}M_{m'j}(\delta_{\alpha\lambda}-\delta_{\beta\lambda})$$
$$\times(\delta_{\alpha'\mu}-\delta_{\beta'\mu}). \tag{B11}$$

Power counting reveals that logarithmic divergencies arise when $l=l'$ and $\alpha=\beta'$ and $\beta=\alpha'$. Thus, with the help of the relations

$$\sum_{l}G^{l}_{m}G^{l}_{m'}=\tfrac{3}{2}|G|^2\delta_{mm'},$$

$$\sum_{l}G^{l}_{m}G^{l}_{m'}(\hat{G}\cdot\hat{k})^2=\tfrac{3}{8}|G|^2(P^{T}_{mm'}+3P^{L}_{mm'}), \tag{B12}$$

we obtain

$$N^{R}_{ij}(k)=N_{ij}(k)+g^2\tilde{a}^4|G|^2T\frac{3\pi}{2}\left(\frac{1}{\mu^2k^2}P^{T}_{ij}\left[I_0(\psi)+\tfrac{1}{2}I_1(\psi)\right]+\frac{1}{(2\mu+\lambda)^2k^2}P^{L}_{ij}\left[I_0(\psi)-\tfrac{1}{2}I_1(\psi)\right]\right)\frac{1}{4\tau}\left[\left(\frac{L}{\tilde{a}}\right)^{4\tau}-1\right]. \tag{B13}$$

Upon projecting out of Eq. (B13) the longitudinal and transverse components, and recalling that $|G|^2T=8\pi\mu(2\mu+\lambda)/(3\mu+\lambda)+O(\tau)$, we finally arrive at the flow equations

$$L\frac{dA}{dL}=g^2\tilde{a}^4\left(\frac{L}{\tilde{a}}\right)^{4\tau}12\pi^2\mu\frac{2\mu+\lambda}{3\mu+\lambda}[I_0(\psi)-\tfrac{1}{2}I_1(\psi)],$$

$$L\frac{dB}{dL}=g^2\tilde{a}^4\left(\frac{L}{\tilde{a}}\right)^{4\tau}12\pi^2\mu\frac{2\mu+\lambda}{3\mu+\lambda}[I_0(\psi)+\tfrac{1}{2}I_1(\psi)]. \tag{B14}$$

APPENDIX C

This appendix details the calculation of the dynamical exponent z. Consider the Langevin equation for the free Hamiltonian H_0 of Eq. (2.14),

$$\gamma\partial_t\vec{u}(\vec{r},t)=-\frac{\delta H_0}{\delta\vec{u}(\vec{r},t)}+\vec{\zeta}(\vec{r},t), \tag{C1}$$

where ζ is a white noise defined by the correlation

$$\langle\zeta_i(\vec{r},t)\zeta_j(\vec{r}',t')\rangle=2D\delta_{ij}\delta(\vec{r}-\vec{r}')\delta(t-t'). \tag{C2}$$

The fluctuation-dissipation theorem insures that thermal equilibrium at temperature T is established for $D=T\gamma$.

Equation (C1) is easily solved. The momentum- and frequency-dependent transverse and longitudinal correlation functions read

$$S_{ij}^{0T}(\vec{k},\omega)\equiv\langle u_i(\vec{k},\omega)u_j(-\vec{k},-\omega)\rangle^T=\frac{2D\gamma^{-2}}{\omega^2+\gamma^{-2}\mu^2k^4}P_{ij}^T,$$

$$S_{ij}^{0L}(\vec{k},\omega)\equiv\langle u_i(\vec{k},\omega)u_j(-\vec{k},-\omega)\rangle^L=\frac{2D\gamma^{-2}}{\omega^2+\gamma^{-2}(2\mu+\lambda)^2k^4}P_{ij}^L. \tag{C3}$$

The presence of an external pinning potential turns Eq. (C1) into Eq. (2.32) by introducing on the right hand side the additional term

$$-\frac{\delta U_{\rm pin}}{\delta\vec{u}(\vec{r},t)}=\frac{2V(\vec{r})}{|\vec{a}\times\vec{b}|}\sum_{l=1}^{3}\vec{G}^l\sin(\vec{G}^l\cdot[\vec{r}-\vec{u}(\vec{r},t)]), \tag{C4}$$

which can be regarded as a perturbation. First order perturbation theory can thus be employed to compute the correlation functions. The perturbation series is found again to diverge logarithmically below T_c. This divergence causes the dynamical exponent to deviate from its mean field value, $z=2$ [22]. To quantify this deviation, consider the transverse correlation function

$$\langle u_i(\vec{k},\omega)u_j(-\vec{k},-\omega)\rangle^T=\frac{1}{\omega^2+\gamma^{-2}\mu^2k^4}[2D\gamma^{-2}P_{ij}^T+P_{im}^TP_{in}^T\overline{\langle\hat{F}_m(\vec{k},\omega)\hat{F}_n(-\vec{k},-\omega)\rangle}]+\cdots, \tag{C5}$$

where the overline indicates averaging over the external pinning disorder, and we have defined

$$\hat{F}_i(\vec{k},\omega)=\int d^2r\int dt\ e^{i\omega t}e^{-i\vec{k}\cdot\vec{r}}\frac{\delta U_{\rm pin}}{\delta u_i(\vec{r},t)}. \tag{C6}$$

Upon carrying out the disorder average, we obtain

$$\overline{\langle\hat{F}_i(\vec{k},\omega)\hat{F}_j(-\vec{k},-\omega)\rangle}=\int dt\ e^{i\omega t}2g\sum_{l=1}^{3}G_i^lG_j^l\langle\cos\vec{G}^l\cdot[\vec{u}(\vec{r},t)-\vec{u}(\vec{r},0)]\rangle. \tag{C7}$$

Noting that

$$\begin{aligned}\langle\cos\vec{G}^l\cdot[\vec{u}(0,t)-\vec{u}(0,0)]\rangle&=\left(\frac{\tilde{a}}{L}\right)^{2-2\tau}\exp\left(\sum_{ij}\int\frac{d^2k}{4\pi^2}G_i^l[S_{ij}^{0T}(\vec{k},t)+S_{ij}^{0L}(\vec{k},t)]G_j^l\right)\\&=\left(\frac{\tilde{a}}{L}\right)^{2-2\tau}\exp\left[\frac{|G|^2T}{8}\int_0^\infty dk\ k\left(\frac{e^{-(\mu/\gamma)k^2|t|}}{\mu k^2}+\frac{e^{(2\mu+\lambda)/\gamma k^2|t|}}{(2\mu+\lambda)k^2}\right)\right]\\&=\left(\frac{\tilde{a}}{L}\right)^{2-2\tau}\left(\frac{\mu}{2\mu+\lambda}\right)^{(1-\tau)\mu/(3\mu+\lambda)}\left(\frac{L^2}{2\sqrt{c}\gamma^{-1}\mu|t|}\right)^{1-\tau},\end{aligned} \tag{C8}$$

and setting $\omega=0$, we arrive at

$$\overline{\langle\hat{F}_i(\vec{k},\omega)\hat{F}_j(-\vec{k},-\omega)\rangle}=2g\tilde{a}^2\frac{3}{2\mu}|G|^2\delta_{ij}\left(\frac{\mu}{2\mu+\lambda}\right)\frac{\mu}{3\mu+\lambda}\frac{2\gamma}{\sqrt{c}}\ln\left(\frac{L}{a}\right)+O(g\tau). \tag{C9}$$

Thus we can write

$$L\frac{dD}{dL}=24\pi ga^2\left(\frac{L}{a}\right)^{2\tau}\sqrt{c}\frac{2\mu+\lambda}{3\mu+\lambda}\left(\frac{\mu}{2\mu+\lambda}\right)^{\mu/(3\mu+\lambda)}\equiv\zeta(g). \tag{C10}$$

The dynamical exponent is determined by the value of $\zeta(g)$ at the fixed point

$$z=2+\zeta(g^*), \tag{C11}$$

leading to Eq. (2.33).

APPENDIX D

The Ornstein-Zernicke theory of hexatics is derived in this appendix. We start from the partition function of the crystal

$$\mathcal{Z}=\int \mathcal{D}[u_1]\mathcal{D}[u_2]\exp(-F/T), \tag{D1}$$

where

$$F=\tfrac{1}{2}\int d^2r(\lambda u_{ii}^2+2\mu u_{ij}^2). \tag{D2}$$

In the presence of dislocations, the displacement field $\vec{u}$ is multivalued; if an arbitrary loop $\mathcal{L}$ encloses dislocations with total Burger's vector $\vec{b}$, then

$$\oint_{\mathcal{L}}\partial_i u_j dx_i=b_j. \tag{D3}$$

It is convenient to express Eq. (D3) in local form,

$$\epsilon_{ik}\epsilon_{jl}\partial_k\partial_l u_{ij}(\vec{r})=\sum_\alpha \vec{b}^\alpha\times\vec{\nabla}\delta(\vec{r}-\vec{r}_\alpha)\equiv S(\vec{r}). \tag{D4}$$

Here we have introduced a source term $S(\vec{r})$ related to the local density of Burger's vectors; it can be easily generalized to include other types of defects, such as disclinations, vacancies, or interstitials [23].

The partition function can now be evaluated as an unrestricted integral over the three independent components of the symmetric strain tensor u_{ij}, provided that constraint (D4) is enforced. This is easily accomplished with the aid of an auxiliary field ψ:

$$\mathcal{Z}=\int \mathcal{D}[u_{11}]\mathcal{D}[u_{12}]\mathcal{D}[u_{22}]\mathcal{D}[\psi]\exp(-F/T)$$
$$\times\exp\left(i\int d^2r\ \psi(r)[\epsilon_{ik}\epsilon_{jl}\partial_k\partial_l u_{ij}(\vec{r})-S(\vec{r})]\right]. \tag{D5}$$

Next we write, as can be most generally done for any symmetric tensor,

$$u_{ij}(\vec{r})=\tfrac{1}{2}(\partial_i v_j+\partial_j v_i)+P_{ij}^T h, \tag{D6}$$

where $v(\vec{r})$ is a single-valued vector (describing, e.g., the small thermal displacements of the atoms from the sites of a randomly distorted lattice), and $h(\vec{r})$ a scalar field, related to the defect density $S(\vec{r})$, in terms of which the constraint enforced by the auxiliary field ψ becomes

$$\nabla^2 h(\vec{r})=S(\vec{r}). \tag{D7}$$

The partition function becomes a functional integral over $\vec{v}$, h, and ψ, and the latter fields can be integrated out easily to obtain the free energy functional

$$\mathcal{F}=\tfrac{1}{2}\int\frac{d^2k}{(2\pi)^2}v_i(-\vec{k})k^2[\mu P_{ij}^T+(2\mu+\lambda)P_{ij}^L]v_j(\vec{k})$$
$$+\lambda\int d^2r(\vec{\nabla}\cdot\vec{v})\nabla^{-2}S(\vec{r})+\tfrac{1}{2}(2\mu+\lambda)$$
$$\times\int d^2r[\nabla^{-2}S(\vec{r})]^2. \tag{D8}$$

This is a rather general expression of the two-dimensional elastic free energy. It allows us to study the effect of both quenched and annealed defects.

First, we consider the effect of annealed dislocations. It is instructive to recast Eq. (D8) in terms of density fluctuation and bond angle variables $\delta\rho$ and θ, respectively, which are related to the divergence and curl of the displacement vector: $\delta\rho=\vec{\nabla}\cdot\vec{u}$, $\theta=\vec{\nabla}\times\vec{u}/2$. Because the displacement vector decomposes naturally into single-valued and singular parts,

$$\vec{u}=\vec{v}+\vec{u}_s, \tag{D9}$$

so do the density fluctuation and bond angle variables:

$$\theta=\theta_0+\theta_s,\quad \delta\rho=\delta\rho_0+\delta\rho_s. \tag{D10}$$

The defect source term $S(\vec{r})$ can be expressed in terms of ρ_s by noting first that, for a distribution of dislocations with Burger vector density $\vec{b}(\vec{r})=\Sigma_\alpha\vec{b}^\alpha\delta(\vec{r}-\vec{r}_\alpha)$ and $S(\vec{r})=-\vec{\nabla}\times\vec{b}(\vec{r})$ from Eq. (D4), and, hence,

$$\nabla^{-2}S(\vec{r})=\frac{1}{1-\sigma}\vec{\nabla}\cdot\vec{u}_s=\frac{\delta\rho_s}{1-\sigma}, \tag{D11}$$

where $\sigma=\lambda/(2\mu+\lambda)$ is the Poisson ratio.

The partition function of annealed dislocations [8] involves averaging over thermally excited Burger's vectors with weight proportional to

$$\exp\left(-E_c\int d^2r\ \vec{b}(\vec{r})\cdot\vec{b}(\vec{r})\right)$$
$$=\exp\left[-E_c\int d^2r\left(4(\nabla\theta_s)^2+\frac{1}{(1-\sigma)^2}(\nabla\delta\rho_s)^2\right)\right]. \tag{D12}$$

Thus, from Eqs. (D8)–(D12), it follows that

$$\mathcal{Z}_{\text{annealed}}=\int\mathcal{D}\delta\rho_0\mathcal{D}\delta\rho_s\mathcal{D}\theta_0\mathcal{D}\theta_s\exp\left(-\frac{\mathcal{F}_{\text{annealed}}}{T}\right), \tag{D13}$$

with

$$\mathcal{F}_{\text{annealed}}=\tfrac{1}{2}\int d^2r[4\mu\theta_0^2+(2\mu+\lambda)(\delta\rho_0)^2]$$
$$+\frac{\lambda}{1-\sigma}\int d^2r(\delta\rho_0)(\delta\rho_s)+\frac{2\mu+\lambda}{2(1-\sigma)^2}$$
$$\times\int d^2r(\delta\rho_s)^2+E_c\int d^2r\left(4(\nabla\theta_s)^2\right.$$
$$\left.+\frac{1}{(1-\sigma)^2}(\nabla\delta\rho_s)^2\right). \tag{D14}$$

Consider now the linear response of the system to a probe coupled to the bond angle. One finds easily that

$$\frac{1}{\mu(q)} = \frac{1}{\mu} + \frac{1}{E_c q^2}, \tag{D15}$$

showing that the shear modulus μ vanishes at long wavelengths for finite E_c (i.e., above the melting temperature). Similar behavior for $\mu(q)$ was found by Marchetti and Nelson in a dislocation loop model of the melted Abrikosov flux lattice [24]. In contrast, the coupling between $\delta\rho_0$ and $\delta\rho_s$ prevents the bulk modulus from vanishing at long wavelengths.

[1] *Physics of Sliding Friction*, edited by B. N. J. Persson and E. Tosatti (Kluwer, Boston, 1996); M. Kardar and D. Ertas, in *Scale Invariance, Interfaces and Non-Equilibrium Dynamics*, edited by A. McKane *et al.* (Plenum, New York, 1995), and references therein.

[2] M. P. A. Fisher, Phys. Rev. Lett. **62**, 1415 (1989).

[3] J. L. Cardy and S. Ostlund, Phys. Rev. B **25**, 6899 (1982).

[4] C. A. Murray, W. O. Sprenger, and R. Wenk, Phys. Rev. B **42**, 688 (1990).

[5] See articles in *Statistical Mechanics of Membranes and Interfaces*, edited by D. R. Nelson, T. Piran, and S. Weinberg (World Scientific, Singapore, 1989).

[6] *Physics of the Two-Dimensional Electron Gas*, edited by J. T. Devreese and F. M. Peeters (Plenum, New York, 1987).

[7] R. Seshadri and R. M. Westervelt, Phys. Rev. B **46**, 5142 (1992).

[8] D. R. Nelson and B. I. Halperin, Phys. Rev. B **19**, 2457 (1979); J. M. Kosterlitz and D. J. Thouless, J. Phys. C **6**, 1181 (1973); A. P. Young, Phys. Rev. B **19**, 1855 (1979). For a recent experimental confirmation of the existence of the hexatic phase, see C.-Y. Chao, C.-F. Chou, J. T. Ho, F. W. Hui, A. Gin, and C. C. Huang, Phys. Rev. Lett. **77**, 2750 (1996).

[9] T. Giamarchi and P. LeDoussal, Phys. Rev. B **52**, 1242 (1995).

[10] L. Radzihovsky and D. R. Nelson, Phys. Rev. A **44**, 3525 (1991).

[11] We are indebted to T. Hwa for discussions on this point.

[12] D. Cule and T Hwa, Phys. Rev. Lett. **77**, 278 (1996); T. Hwa (private communication).

[13] C. Carraro and D. S. Fisher, Phys. Rev. B **51**, 534 (1995).

[14] D. R. Nelson and S. Seung, Phys. Rev. B **39**, 9153 (1989).

[15] L. D. Landau and E. M. Lifshitz, *Theory of Elasticity* (Pergamon, New York, 1970).

[16] Y. Y. Goldschmidt and A. Houghton, Nucl. Phys. B **210**, 155 (1982).

[17] D. R. Nelson, Phys. Rev. B **27**, 2902 (1983).

[18] J. Toner and D. P. di Vincenzo, Phys. Rev. B **41**, 632 (1990); T. Hwa and D. S. Fisher, Phys. Rev. Lett. **72**, 2466 (1994).

[19] Y.-C. Tsai and Y. Shapir, Phys. Rev. Lett. **69**, 1773 (1992).

[20] D. C. Morse, I. B. Petsche, G. S. Grest, and T. C. Lubensky, Phys. Rev. A **46**, 6745 (1992).

[21] See, e.g., E. Granato, M. R. Baldan, and S. C. Ying, in *The Physics of Sliding Friction*, edited by B. N. J. Persson (Kluwer, Dordrecht, 1995).

[22] R. Bausch, H. K. Janssen, and H. Wagner, Z. Phys. B **24**, 113 (1976).

[23] C. Carraro and D. R. Nelson, Phys. Rev. E **48**, 3082 (1993).

[24] M. C. Marchetti and D. R. Nelson, Phys. Rev. B **42**, 9938 (1990).